Tailoring Highly Ordered Honeycomb Films Based on Ionomer Macromolecules by the Bottom-Up Approach

Laurent Billon,*,† Maggy Manguian,†,‡ Virginie Pellerin,† Mathieu Joubert,†,‡ Olivier Eterradossi,‡ and Hélène Garay‡

Institut Pluridisciplinaire de Recherche sur l'Environnement et les Matériaux, Equipe Physico-Chimie des Polymères IPREM/EPCP CNRS UMR 5254, Université de Pau et des Pays de l'Adour, Hélioparc Pau Pyrénées, 64012 Pau Cedex, France, and Centre de Matériaux de Grande Diffusion, Ecole de Mines d'Alès, 2 avenue Angot, 64053 Pau Cedex 09, France

Received September 12, 2008; Revised Manuscript Received November 11, 2008

ABSTRACT: A novel route to obtain highly ordered self-assembled honeycomb films has been investigated by a bottom-up process. A polymer with one chain end ionic functionality has been synthesized in a one-step reaction by nitroxide-mediated polymerization. This ionomer synthesis represents a very simple way, and honeycomb structured films have been observed after solvent evaporation in a long-range distance of few hundred microns in a very regular ordered arrangement. These films are simply prepared by spreading out polymers CS_2 solutions without additives over various substrates as well on inorganic surfaces as onto different polymeric substrates such as flexible PVC sheet or rigid PMMA plate. Different experimental parameters, such as polymer concentration or wet thickness, have been checked to tune the pores size and thus the honeycomb morphologies. An elegant technique based on reflected and transmitted light has been used to correlate the pores size inside and on the top of the film. This highly ordered hexagonal pattern on the polymeric surfaces suggests the possibility of taking advantage of the microtextures for inducing optical interferences but also to modify the color of this bioinspired material as a function of their visual angle as in nature.

Introduction

The origin of functional materials in nature is attributed to the presence of highly structured or ordered arrangements. The physical understanding of such organization can lead to original ideas for the creation of new materials exhibiting functional biomimetic properties, especially fascinating optical phenomena such as the nacre or interferential effect, which can be observed in shellfishes or insect wings, respectively. These interferential colors can be obtained by different physical processes such as light diffraction due to highly structured systems or by light multireflection created by superposition of thin homogeneous layers with different refractive indexes. Moreover, we have here to distinguish two optical phenomena based on light diffraction (as gratings) or creation of discrete stop bands (as photonic crystals), called iridescence or opalescence, respectively. The nature is very astonishing when it uses the second one, and some insects generate only one or two pure colors by opalescence with an organization at the nanoscale, i.e., 100 nm. Honeycombs (HC) or breath figures (BF) are generally iridescent, but they could generate opalescence if we would be able to organize them into a very well ordered three-dimensional array 3D with diameter smaller than about 300 nm.

Nevertheless, the honeycomb 2D structured film is one of the most fascinating structures among different highly structured systems which can be obtained by simple polymer solution evaporation. These structures have attracted considerable attention over recent years due to their potential applications in diverse areas such as membranes, photonic or electrophotonic devices, tissue engineering, and catalysis.[1] François et al. have first reported a dynamic approach to prepare highly ordered microporous films with hexagonal array by casting a polymer solution under humid air flow. The condensed water droplets caused by rapid cooling due to the solvent evaporation act as the template that direct the formation of ordered microporous film. They found the honeycomb morphologies were obtained with polystyrene (PS).[2] Nevertheless, all the PS solutions cannot be transformed into honeycomb-like films. François et al. have demonstrated that one of the most important conditions must be the architecture of the macromolecular species present in solutions: they must exhibit chemical or physical starlike structures when PS with low molecular weight around 10K g mol^{-1} is used. Then, either chemical stars PS or polymers able to form starlike micelles by autoassociation must be used. For example, PS-*b*-PPP copolymers lead to such organized films because in solution the insoluble PPP blocks are trapped into micelles cores surrounded by PS corona.[3]

Since these first works, many other polymers have been used such as functional linear polymers,[4] starlike polymers,[5] amphiphilic copolymers,[6] semiconductor polymers,[7] organic/inorganic hybrid complexes,[8] and surfactant-encapsulated clusters.[9] On the other hand, so far, few solid substrates have been reported mica,[10] glass slides,[10] gold or CdSe nanoparticles self-assembly,[11] piezoelectric substrates,[12] or liquid interface as water.[13]

Although a large variety of polymer architectures have successfully been used in the preparation of breath figure patterns, their different structures involve a complex synthetic methodology. Moreover, if no special architecture of the polymer involved has been shown in many papers since the first work of Francois et al., it seems that for linear PS the molecular weight (MW) and the end-functionalization are key parameters influencing the honeycomb (HC) formation.[14]

Indeed, if many linear PS have been used, some distinctions on the HC formation effectiveness can be mentioned. For simple linear PS, the most favorable MW is in the range of 100K−200K.[15] When lower or higher MW is used, films can be observed with large defect pores spread throughout the film and small domains of uninterrupted ordering as in breath figures arrangement (BFA).[14−16] Otherwise, if some polar groups, i.e.,

* To whom correspondence should be addressed. E-mail: laurent.billon@univ-pau.fr.
† Université de Pau et des Pays de l'Adour.
‡ Ecole de Mines d'Alès.

10.1021/ma8020568 CCC: $40.75
Published on Web 12/11/2008

Scheme 1. α-Carboxylic Polystyrene (PS-COOH) Synthetic Procedure by Nitroxide-Mediated Polymerization Initiated with MAMA

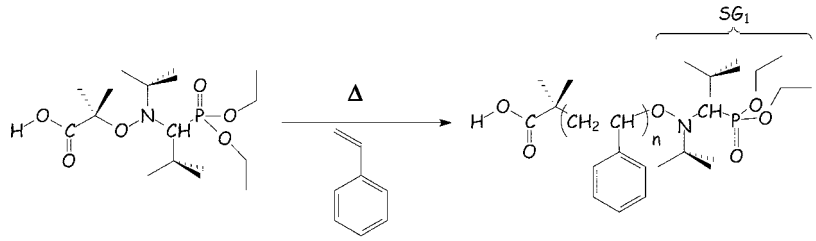

carboxylic acid (COOH), are introduced as an end-functionalization, highly ordered patterns in a long-range distance can be observed for HC structured films as described by Srinivasarao et al.[17] or Bolognesi et al.[16] for PS-COOH 50K and 100K/200K, respectively. In the same time, Kim et al. did not observed for PS-COOH of 30K the formation of HC films but rather breath figure (BF) patterned films presenting nonuniform pore sizes and long-range organization.[18] In all cases, the MW and polar group end-functionalization of PS are associated with the tune of an appropriate viscosity and surface energy, respectively. Moreover, Rawlett et al. recently mentioned that the enhanced arrangement of the pores in the carboxy-terminated PS over nonfunctionalized PS may be attributed to the aggregation of polymer chains; aggregation of end-groups leads to an effective increase in polymer MW and thus viscosity. Moreover, this self-assembly could contribute to stabilizing forces at the polymer/water droplet interfaces.[14] Finally, Srinivasarao et al. mentioned that the polar group for PS-COOH for a low MW (50K) is a necessary condition to obtain an ordered pattern of well-organized spherical cavities on the film surface, as HC highly ordered film.[17]

That is why, in a first step, we were interested by a facile way to produce low-MW PS having a polar chain end functionality. Then in a second time, to extend the area of applications of honeycomb films, we have tested organic polymer surfaces such as substrates. Indeed, we have chosen organic substrates such as poly(vinyl chloride) (PVC) sheets and poly(methyl methacrylate) (PMMA) plates because they presented some strong interests for functional coatings and optical applications. Recently, we have demonstrated that honeycomb-like structured polymer films can reproduce nature by creating an optical interferential and iridescent material, but also significantly increasing the hydrophobicity.[19] This approach could offer new fascinating applications as original biomimetic coating onto polymeric surfaces.

Here, we reported a very simple method to form ordered structures in a long-range distance on various substrates, especially functional polymeric substrates, by synthesizing a monochelic polymer[20] in a one-step process via nitroxide-mediated polymerization. Few experimental parameters have been checked to control and tuned the films morphology to create not only structured surfaces but also thin structured films in 2D and 3D, respectively, by the bottom-up approach. The aim of this paper is to focus a new chemical approach and tune the morphology of BF patterned films in 2D or 3D for creating iridescence as interferential optical phenomena by modeling the polymer architectures and organization. Such an approach, based on bioinspired materials as in butterfly wings, presents the ability of soft matter to create highly ordered structures as functional biomimetic materials.

Experimental Section

Ionomer Macromolecular Synthesis. Nitroxide-mediated polymerization of styrene was performed in bulk with MAMA as initiator to synthesize an α-carboxylic polystyrene (PS-COOH) (Scheme 1).

In a round-bottom flask, 10 g of styrene (8.74 mol L^{-1}) and 0.11 g of MAMA (0.026 mol L^{-1}) were incorporated. Styrene (St, Acros, 99%) and the alkoxyamine 2-methylaminoxyproponic-SG1 (BlockBuilder, Arkema 99%, so-called MAMA) were used as received. The flask was sealed with a septum. The solution was degassed by nitrogen bubbling under stirring for 30 min at room temperature. The flask was immersed into an oil bath at 120 °C for 4 h. After polymerization, the reaction mixture was cooled and diluted with dichloromethane. The polystyrene was recovered by a first precipitation in ethanol, followed by a precipitation in a ethanol/basic water (90/10) mixture in order to obtain the polymer with anionic end-chains (Scheme 2).

Conversion was 56% (determined by ^{1}H NMR analysis of a crude sample in $CDCl_3$ in a 5 mm diameter tube using a AM400 Bruker Advanced spectrometer operating at a frequency of 400 MHz), and the recovered polystyrene had $M_n = 22\,300$ g mol^{-1} and $M_w/M_n = 1.13$.

Nuclear Magnetic Resonance Spectroscopy (NMR). Conversion of styrene and presence of the ionic end-group were determined by ^{1}H and ^{13}C NMR in $CDCl_3$ on a Bruker 400 MHz instrument at room temperature, respectively.

Size Exclusion Chromatography (SEC). Molar mass and molar mass distributions of PS samples were determined at 40 °C using size exclusion chromatography (SEC). Characterizations were performed using a 2690 Waters Alliance system with THF as eluent at a rate of 1 mL/min. The chromatographic device was equipped with four Styragel columns HR 0.5, 2, 4, and 6 working in series at 40 °C, a 2410 refractive index detector, and a 996 Waters photodiode array detector. A calibration curve established with low polymolecularity index polystyrene standards, and toluene was used as an internal standard for the system.

Differential Scanning Calorimetry (DSC). Glass transition temperatures (T_g) were measured using a differential scanning calorimeter (TA series Q100). Samples (~3 mg) were weighed and scanned at 15 deg/min from 20 to 130 °C under dry nitrogen (50 mL/min). The reported values of T_g were determined from the second heating run and were taken as the middle point of the $\Delta H/\Delta T$ step in the DSC spectra.

Film Preparation. Polymer was end-capped by a anionic function, and the ionomer behavior formed stars in the solvent carbon disulfide (bp = 46 °C) due to the nonsolubility of the ionic end-chains. CS_2 solutions of ionomer were spread over mica, poly(methyl methacrylate) (PMMA), and poly(vinyl chloride) (PVC) surfaces. The solution was evaporated at room temperature under hood air flow (moist air) to form highly structured films. When some specific parameters are checked as described in this study, the coatings were performed in a temperature/humidity well-controlled box with "doctor blade" applicator to elaborate reproducible films of a few cm^2.

Observation of Surface Morphology and Film Cross Section. The observation of surface morphology and the microporous films were characterized by optical microscopy (Axiotech, Zeiss) and scanning electron microscopy (SEM, Oxford Instruments, INCA ENERGY 350).

Interferential Optical Properties by Spectrogoniometry. The diffracted luminous intensities by highly structured honeycomb films were measured in both reflection and transmission in the 380−780 nm range, using a goniospectroradiometer (MAS40 CCD array

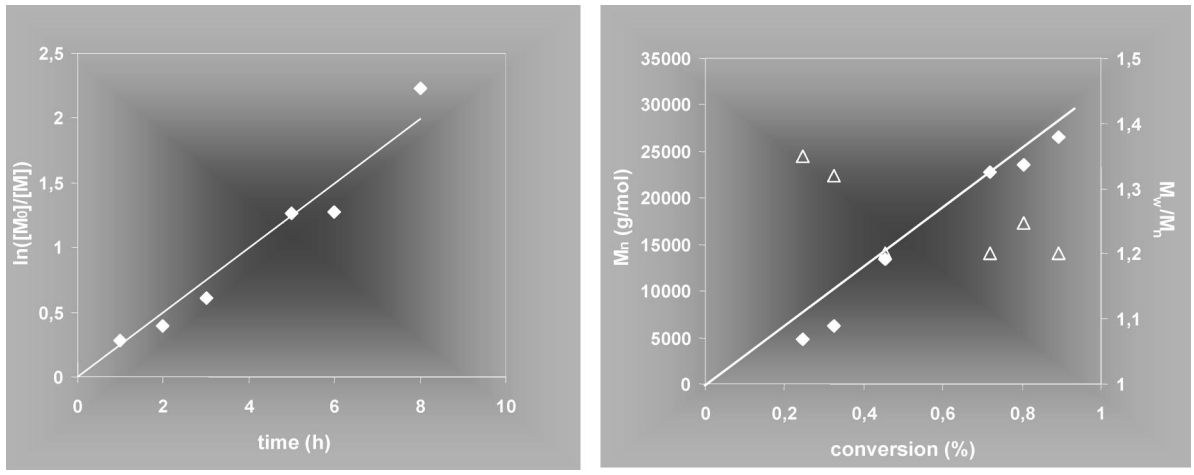

Figure 1. (a) Evolution of $\ln([M]_0/[M])$ vs time and (b) evolution of M_n vs conversion and I_p vs conversion of the polymerization of styrene (S) carried out at 120 °C in the presence of MAMA ([S]/[MAMA] = 330 as straight line).

spectrometer and GON360 goniometer, Instrument Systems) under white halogen illumination. The illumination angle α was set to +10° and 0° from the sample's normal for transmission and reflection, respectively. Reflected light was recorded at angle β ranging from −3° to −87° in 3° steps. For transmitted light, β ranged from 0° to −56° in 2° steps.

Results and Discussion

A Simple Approach to Ionomer Macromolecular Synthesis. The ability of MAMA to initiate and to well-control macromolecular designs, such as statistical, diblock, and gradient copolymers or also ionomers, has been recently demonstrated by Karaki[21] and Ghannam,[22] respectively. This polymerization process permits to accede to macromolecular structures and target desirable molecular weight with low polydispersity. Herein, the well-control of the polymerization process is described by the linearity observed in the plots of the logarithmic change of the monomer concentration with time which indicated not only a first order with respect to the monomer, but that the growing radical concentration remained constant, which was ratified by the linear dependence of M_n with conversion and low values of the polydispersity (Figure 1).

The resulting polymers have a molecular weight and a polydispersity as low as expected for a controlled process. In the present study, the used PS has a molecular weight value $M_n = 22\,300$ g mol^{-1} and a very low polydispersity $I_p = M_w/M_n = 1.13$ after precipitation. Using the MAMA as initiator, the polymer chains are end-functionalized by a carboxylic group from in the initiator site.[21] Here, we have to remind that Kim et al. did not observed for PS-COOH 30K the formation of HC films but rather BF patterned films presenting nonuniform pore sizes.[18] On the other hand, HC structured films, as a highly ordered patterns in a long-range distance, have been observed by Srinivasarao et al.[17] with PS-COOH 50K (higher MW) associated with a viscosity increase.

For a lower MW, as used in this study, this carboxylic acid end-group allows generating an anionic end-functionality, giving it an ionomer group by pH adjustment and thus increasing the polar and the amphiphilic character of the macromolecular chains. That is checked by ^{13}C NMR analysis by the shift of the peak at 182 ppm (Figure 2).

Two-Dimensional Observation of Honeycomb Microstructured Films. François et al. have demonstrated that one of the most important conditions to create highly structured honeycomb PS films by the bottom-up approach is the architecture of the macromolecular species present in solutions: they must exhibit chemical or physical starlike structures due to the nonsolubility of one part of the macromolecule. Moreover, they have just determined an upper limit around a MW of 10K, which means that no HC structured films were observed with very low MW.

As demonstrated by Eisenberg et al., ionomer macromolecules are able to form stars in the organic solvents due to the nonsolubility of the ionic end-chains.[20] They have pointed out the possible self-assembly of carboxylate-terminated monochelic polystyrene and determined by light scattering in different organic solvent, the aggregation number N_{agg}. For the same ionomer PS molecular weight with sodium as counterion, as used in the present study, they determined the formation of micelles at very low concentration ($C_p = 10^{-6}$ mol/L$^{-1} \approx 2 \times 10^{-2}$ g L^{-1}) with an aggregation number N_{agg} varying from 13.5 to 16.6 in CCl_4 and cyclohexane, respectively. We have tried to determine the aggregation number N_{agg} for sodium carboxylate-terminated monochelic PS by static light scattering. We obtained apparent MW values in the range of 240 000−320 000 g/mol for the same polymer in CS_2 solvent. This values range is due to the high volatility of this last one which modifies the polymer concentration and thus the calculated value of the apparent MW. Nevertheless, these values have to be corrected from the polydispersity of the polymer used herein, i.e., 1.13. Because of the unimer MW around 22 000 g/mol, the N_{agg} calculated value can be estimated around 10 in CS_2, a solvent with higher polarity than CCl_4 as cyclohexane.

In the present study, we have used this ability of ionomer macromolecules based on low-MW PS to self-assemble in organic solvent to form starlike micelles by autoassociation of the ionic end-group. Here, CS_2 (bp = 46 °C) solutions of ionomer ($C_p = 10$ g L^{-1}) were spread over an inorganic (mica) or polymeric (poly(vinyl chloride) (PVC) sheet, PMMA plate) surfaces. The solutions were evaporated at room temperature just under hood air flow with air humidity 85% to form a film and condense water microdroplets onto the drying polymer solution in CS_2. The evaporation of water droplets involves the formation of micropores in a hexagonal network.[1−19]

Few studies have been focused on the influence of substrates on the honeycomb pattern formation. In most cases, mica, glass slides, or metal material have been used. Cheng et al. have investigated the influence of the substrate on the formation on the honeycomb structure by using an amphiphilic dendronized block copolymer.[10] Three solid substrates have been checked mica, glass slide, and silicon plate. They claimed that mica was the most suitable substrate among them to form orderly porous films. Indeed, it was impossible to prepare ordered porous films on the silicon plates under identical conditions.

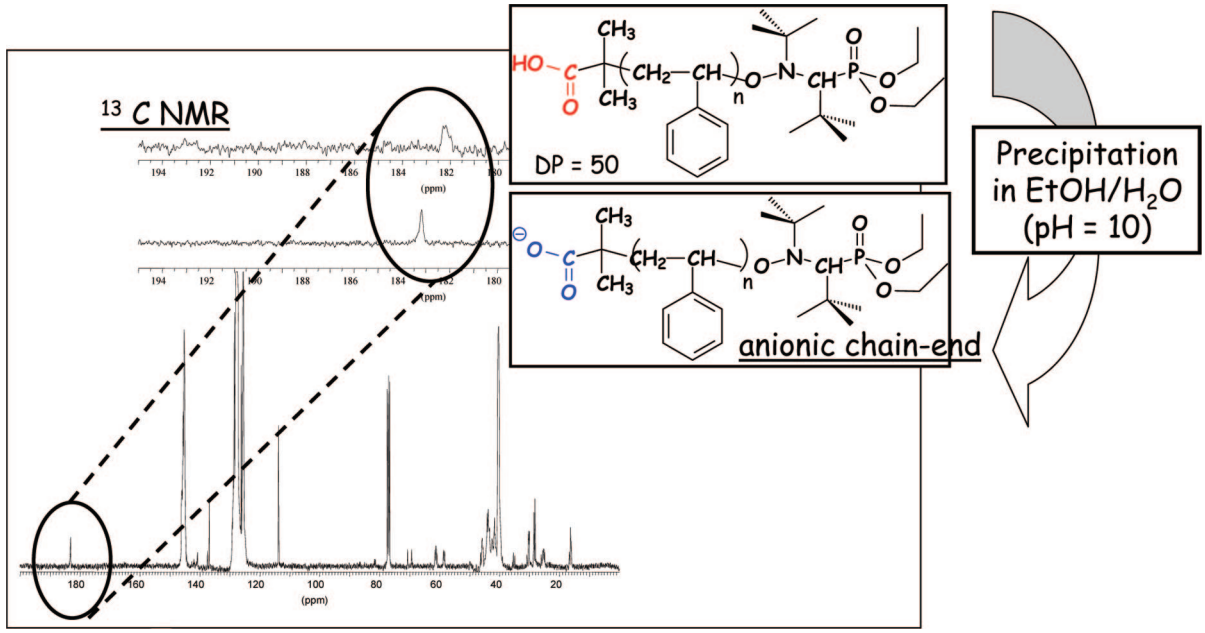

Figure 2. ^{13}C NMR of polystyrene in $CDCl_3$ before and after the second precipitation in a ethanol/basic water mixture in order to form the ionomer structure (polystyrene (PS) with low polymerization degree was analyzed to see the chain ends; $DP_n = 50$).

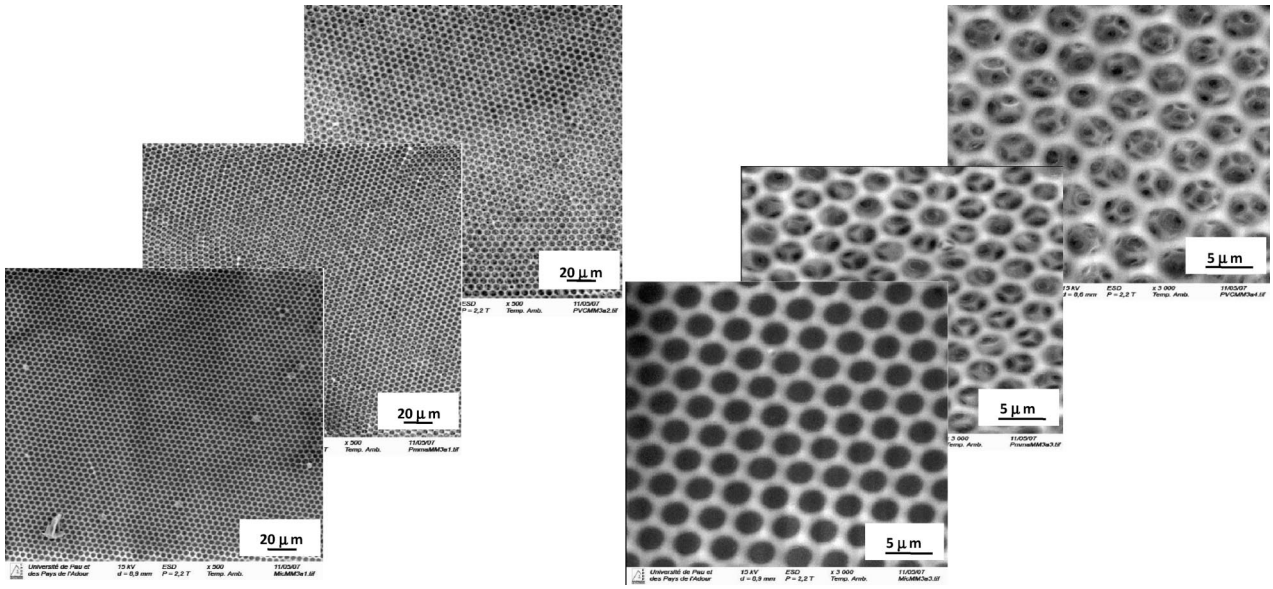

Figure 3. SEM images over various surfaces PVC sheet, PMMA plate, and mica, from a polymer solution concentration $C_p = 10$ g L^{-1}, from top to bottom, respectively. Left scale bar = 20 and right scale bar = 5 μm.

So, one important challenge was to reproduce these organized structures on organic surfaces and especially polymeric substrates. Poly(vinyl chloride) (PVC) sheets and poly(methyl methacrylate) (PMMA) plates have been used as substrates for the first time. As shown in Figure 3, highly ordered structures in a hexagonal array in a long-range distance, i.e., honeycomb (HC) structured film, is observed as well on PVC sheet as on PMMA plate.

The size of the pores was found very homogeneous and around 3 μm of diameter for the same polymer concentration. The solutions were evaporated at room temperature just under air flow of the hood to form a film (air humidity 85%). However, if the same concentration of polystyrene solution was used for fabrication porous films, we have found some difference on the self-assembly behaviors probably caused by the various surface properties of PVC and PMMA substrates. It can be observed that the size of the pores on PVC is obviously slightly bigger than that on PMMA. In order to check the effect of the surface properties, such as polarity or dielectric properties of different polymeric substrates, studies are still underway.

The domain of applications of these films is very large and has still to be explored, especially toward functional coatings. Indeed, we recently demonstrated the ability of such structured surfaces to create highly ordered films on inorganic substrates using ionomer macromolecular design. An original property of these films with an iridescent color obtained by light diffraction as a result of the optical interferences of sunlight with the periodic honeycomb structures was presented.[19] All these new materials based on polymeric controlled structures can reproduce nature by creating an optical interferential and iridescent material associated with an increase of the hydrophobicity, which offers new fascinating applications as original biomimetic coatings on flexible polymeric substrates.

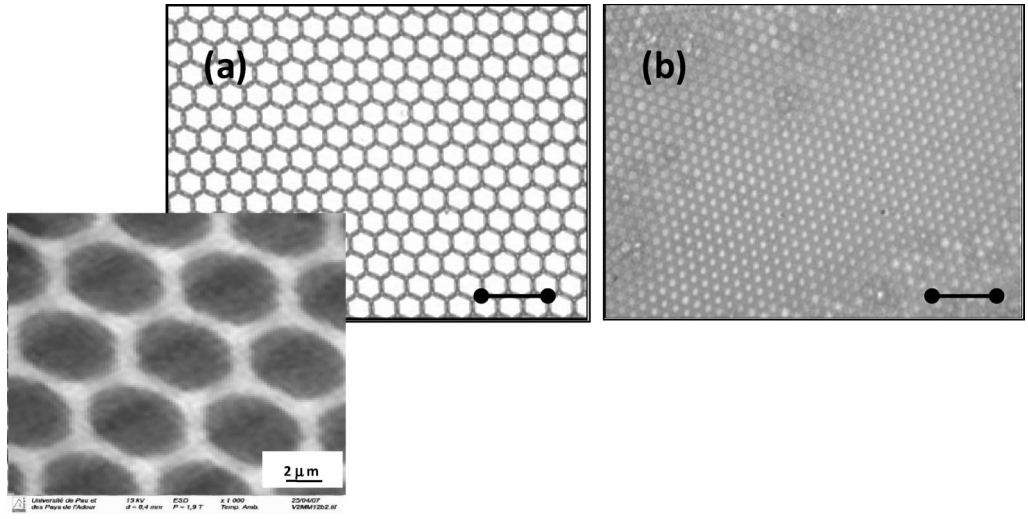

Figure 4. SEM image (scale bar = 2 μm) and optical micrographs of polystyrene honeycomb structures on mica substrate with different polymer solution concentrations C_p = (a) 1.2 and (b) 10 g L^{-1} (scale bar = 20 μm).

Tuning the Pores Size of Surface. The pore diameters of honeycomb films can be easily influenced by several parameters such as the humidity, the polymer structure, the molecular weight of the polymer, the concentration of the polymer solution, or the air flow velocity. As shown in Figure 4, the pore size can be tuned with the concentration of the polymer when the film is strictly prepared in the same conditions.

An increase in the concentration of the polymer results in a decrease in the pore size. The pore diameter is 6.6 μm for a concentration of 1.2 g L^{-1}, whereas it is 3 μm at 10 g L^{-1}. This strong increase of the pore diameter is accompanied by the formation of a monolayer as observed in SEM image (Figure 4). The formation of such a film could be due to the low polymer concentration stabilizing large water droplets which are able to connect and adhere to the hydrophilic mica surface after dipping in the polymer solution. The pore diameter determine by SEM is relatively closed to the optical value, i.e., 5.9 μm.

Stenzel et al. explained the increased capacity of the polymer to stabilize a larger surface area of the water droplets before the precipitation of the polymer around the water droplet.[23] The authors observed a correlation between the pore size and concentration. The origin of the formation of honeycomb polymer films from organic solution is considered as the condensation of microdroplets of water due to evaporation of the organic solvent to subsequent cooling of the solution, as described the first time by François et al.[2] They claim that droplets are at the surface and are prevented from coalescence by the formation of a layer of precipitated polymer around droplets. This so-called "polymer bag effect" can almost be seen in few studies.[24] Bunz considers that this "polymer bag effect" or the encapsulation of the droplets must be important in the final stages of the process.[1] Moreover, Karthaus considers, as François et al., that the initial water droplets neither levitate nor are ordered at the surface, and thermocapillary and Marangony forces alone are responsible for the formation of a hexagonal array.[25]

Here, the origin of the bag effect could be due to the precipitation of a thin rigid polymer film, previously adsorbed at the water/CS_2 interface. This ability corresponds to an amphiphilic polymer behavior of ionomer structures. Indeed, in the case of ionomers, this antagonist solubility is due to a partial affinity of the polymer for water. When polymer is adsorbed at the water/CS_2 interface, the anionic end-groups could emerged in water, and the contacts between water and the main polymer chain induce its precipitation and the "bag" formation. This mechanism is compatible with the process

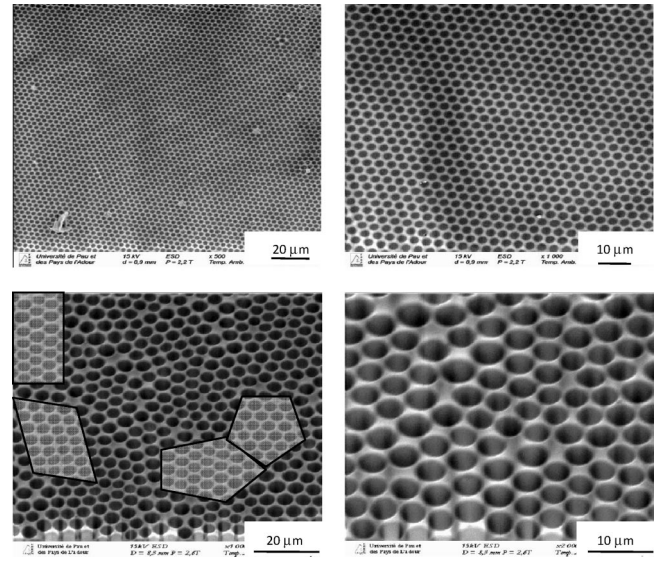

Figure 5. SEM images of HC structured film obtained with PS-COO^-Na^+ (top) and BF patterned film with PS-COOH (bottom) from C_p = 10 g L^{-1} over mica at room temperature under hood air flow and 85% of humidity (left and right scale bars are 20 and 10 μm, respectively).

describes by Karthaus[25] and Srinivasarao[17] which mention that a crucial point is the prevention of the coalescence of the water droplets. In this case, the water droplets would have no time to coalesce during and before the complete evaporation of the solvent due to the bag effect, i.e., formation of a solid thin polymer film at the interface water/CS_2.

At this stage, it is important to note that no highly ordered organization in a long-range distance as honeycomb structures was observed from the "protonated" PS-COOH 22K under our experimental conditions. We have just observed films with large defect pores spread throughout the film and limited domains of uninterrupted ordering (Figure 5).

Here, the difference between BF patterned (bottom) and HC structured (top) films is observed when pores with a lower or higher size come to introduce a defect in the organization of monodisperse pores. Indeed, as shown in Figure 5 (gray zones), delimited HC structured domains are formed and surrounded by different pores size which rapidly denature the perfect organization in a long-range distance. Bolognesi[16] and Rawlett[14] mentioned the self-organization of PS-COOH with highest

Scheme 2. Schematic Representation of the Formation of the Honeycomb Structured Films by Ionomer-Stabilized Condensed Water Droplets

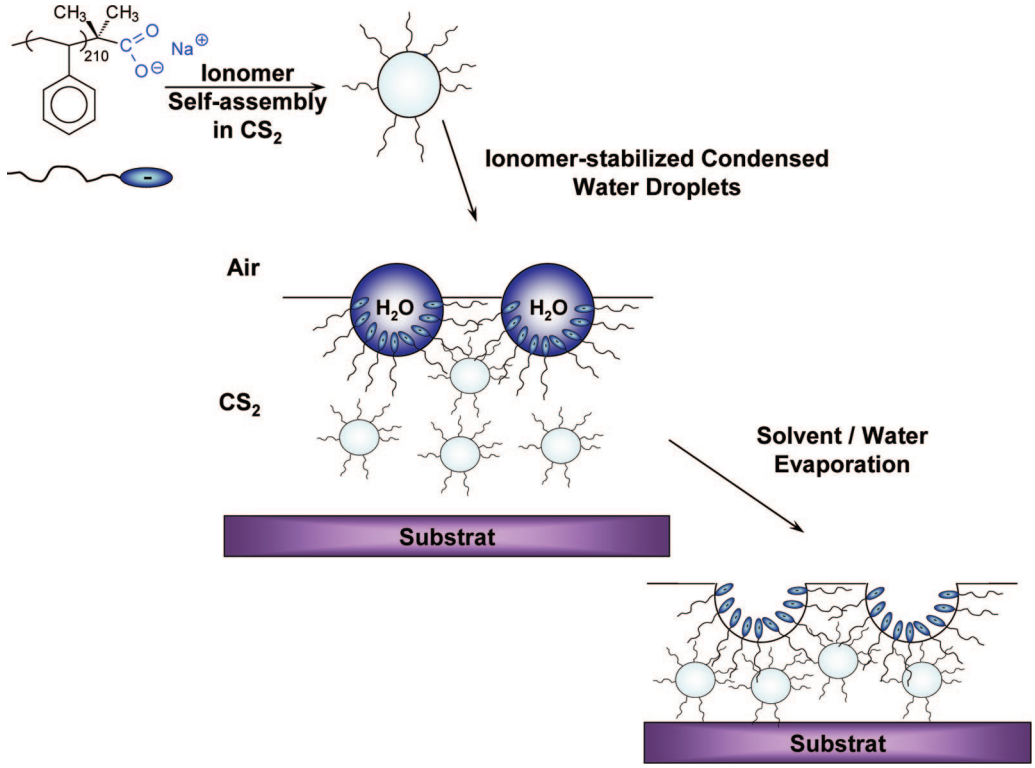

molecular weight (M_n = 100K), without specific attention to the chemical nature of the end-group ("protonated" group COOH or sodium acrylate group COO^-Na^+). In the present case for lower MW of PS, the impact of the ionization of the carboxylate-terminated monochelic PS macromolecules could have an important role on the supramolecular self-assembly in solution[20] or in bulk[26] and also on the final properties of such assembly to form HC structured films. Indeed, Eisenberg et al. have shown the viscosity of PS- COO^-Na^+ in toluene is significantly higher than that of PS-COOH, which indicates clearly the formation of multimers in the sodium carboxylate-terminated polystyrene, associated with the formation starlike polymers. One feature of these materials is that the ionic groups aggregate into ionic domains, which effectively cross-link the polymer chains into resulting networks when concentration increases.[26] This lost of mobility has been also reported by a ^2H NMR study of the chain dynamics in coronas of ionomer aggregates.[27] The authors found that the mobility of styrene segments close to the micellar cores is reduced significantly. Styrene segments 20 repeat units away from the nonionic−ionic block junction can still "feel" the restriction imposed by the ionic cores, behaviors which support the ionomer model based on the mobility reduction in the vicinity of ionic multiplets.[28] The highest initial viscosity due to the starlike micelles associated with the progressive increase of viscosity, i.e., progressive formation of the network during the solvent evaporation, could confirm the ability of the ionomer macromolecules to act as a stabilizer of the water droplets. Water droplets could be stabilized by surface-active compounds, i.e., ionomers as amphiphilic molecules with hydrophilic head (COO^-) and hydrophobic tail (PS), which could be located at the water/CS_2 interface, as represented in Scheme 2. This schematic representation could leave to functionalized surface of the inner pores or cavities. Such a final stage has been recently observed with a polar end-group or with amphiphilic copolymers. Indeed, Yunus et al. demonstrated by TOF-SIMS the presence of the polar groups within the extreme surface of the cavities.[24] Stenzel et al. used amphiphilic block copolymer based on acrylic acid (AA), i.e., PS-*b*-PAA, to stabilize water droplets and obtain HC structured films. In this case the hydrophilic acrylic acid groups are located on the pore surface and after their postfunctionalization with streptavidin used for specific proteins adhesion.[29]

Moreover, for the present low MW PS-COO^-Na^+, it seems that ionomers prevent coalescence and lead to monodisperse water droplets size (Figure 5, top). Indeed, a very regular pore size is observed attributed to the evaporation of uniform water droplets strongly stabilized by amphiphilic macromolecules. On the contrary, PS-COOH does not form highly structured films due to the coalescence or to different size of condensed water droplets (Figure 5, bottom). Such phenomena could be due to the increase of the polar or "amphiphilic" behavior of ionized COOH end-functionalized PS, behaving as a stabilizer of the water/CS_2 interface and preventing coalescence.

As we demonstrated in a recent study for a "soft" polymer with a glass transition temperature T_g below the room temperature, the same mechanism appears. Initially, in the formation of microsized water bubbles at the surface of the film and finally at the end of the evaporation process (evaporation of both CS_2 and water), the water droplet template disappears and a homogeneous film without pores is observed. This behavior was due to the creep of the elastomer polymer inside pores.[19] Here, we use a "hard" thermoplastic PS to avoid such phenomena, but in the final stage, when CS_2 is totally evaporated, another interesting behavior of such ionomers in bulk can be described. Indeed, based on the ionomer model, the restricted mobility is also present in polymer melt or bulk.[27,28]

We have thus studied by DSC the impact of the macromolecular design on the T_g values of the self-assembly in bulk (Table 1).

Three different types of PS macromolecular design with equivalent MW have been synthesized by nitroxide-mediated polymerization using SG1 as counter radical and analyzed by

Table 1. Impact of the Macromolecular Design on the T_g Values of the Self-Assembly in Bulk

	macromolecular characteristics			DSC thermal property		
	end-group functionality	M_n (g mol^{-1})	I_p	T onset (°C)	T_g (°C)	ΔC_p (J/(g °C))
PS-COOH	neutral	22 300	1.13	89.1	92.8	0.285
PS-COO^-Na^+	anionic	22 300	1.13	102.1	104.1	0.237
PS-$C(NH_2)=NH_2^+Cl^-$	cationic	24 000	1.23	102.9	105.7	0.279

DSC. For neutral end-functionality, we observed a classical thermal behavior of the PS chains as a function of the molecular weight. Here, we calculated a lower value of the T_g compared to the classical value for high-MW PS around 100 °C. Indeed, in this range of molecular weights, the longer the chains, the higher the T_g values are. When an ionic functionality is introduced as an end-group, we observed an enhancement of the T_g values of more than 10 °C in bulk. This behavior can be directly correlated with the self-assembly of the ionic group in clusters to reinforce the thermal properties of the PS chains.[27,28] For the same molecular weight, but with two different groups, i.e., anionic or cationic, the same T_g values have been observed, demonstrating thus the impact of the macromolecular design on the mobility and the thermal property of the PS ionomer chains. The ionic aggregates behaves as cross-linker agents which significantly decrease the PS chains mobility and increase the viscosity which could encourage the "bag effect" and prevent the water droplets coalescence in the final stage of the evaporation for low PS molecular weight (MW).

Moreover, if the highly ordered hexagonal array is observed in a long-range distance when different polymer concentrations are used, the dimensions of the holes are very different: 3 times higher for the lowest concentration as shown in Figure 4. This could mean that in the first stage of the evaporation the size of the stabilized microdroplets of water is different. This behavior is probably due to the concentration of surface-active compounds, i.e., ionomers as amphiphilic molecules or macro surfactants, which modify the tension surface energy. When the concentration is high (above the cmc $\approx 10^{-6}$ mol L^{-1}),[15] the number of macrostabilizers increases, and they could stabilize a larger surface area and thus higher number of smaller condensed water droplets onto the CS_2 surface.

Tuning the Honeycomb Films Morphologies. Another interesting experimental parameter for changing the honeycomb morphology is the wet thickness of the polymer solution. The wet thickness is defined as the height of the polymer solution casted on the substrate (Figure 6).

For a low wet thickness casts on the mica substrate, we have observed the formation of a monolayer as described in a previous section. When we casted a higher wet thickness on the substrate from 250 to 500 μm, we observed the partial formation of a second structured layer on the top of the first one, with a shift of a half-periodicity of the hexagonal arrays. The wet thickness has been thus increased up to 1000 μm to form in a long-range distance a "perfect" double-layer of self-assembled pores in a hexagonal pattern. Such behavior could be due to two successive condensations of water droplets at the polymer solution/air interface, inducing the dive of the first layer or their self-organization into the solution in a highly ordered hexagonal array. Indeed, if the wet thickness of the dropped off polymer solution is sufficiently important, the formation of a multilayered honeycomb structured film seems to be addressed. Such a phenomenon could be due to the Bènard−Marangoni convection and thermocapillary effects which forced the water droplets circulation inside the thickness of the polymer solution. Indeed, when a first layer of condensed water droplets is formed on the top of the solution, these last ones could dive inside the solution dragging down by the thermal convection flow and pushed away by a new layer of condensed water droplets. A tentative of schematic representation of the multilayered honeycomb structured film will be described later on (Scheme 4). This mechanism is not really well understand until now, but it seems correlated to a complex conjuncture between the value of the wet thickness and also the evaporation speed which have to be sufficiently slow to permit the dive of a first water droplets layer and a new water droplets condensation on the top of the evaporating polymer solution. However, the cross-section observation by microscopy of such mono- or double-layered structured films is proved too difficult due to their weakness, even when the film is still coated on the substrate.

Honeycomb Films Cross-Section Observation. As demonstrated in the previous section, the thin honeycomb films are very difficult to be manipulated or optically analyzed. Few films

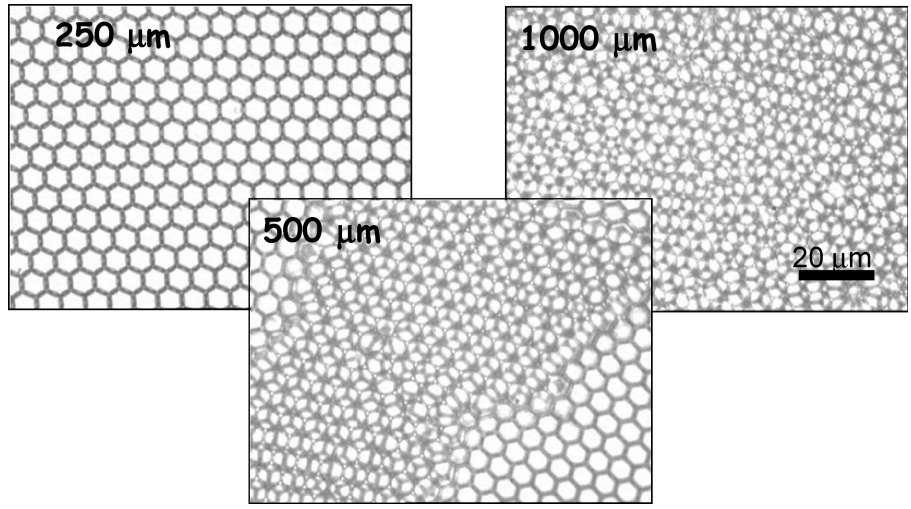

Figure 6. Optical images of honeycomb morphologies from a PS solution concentration $C_p = 1.2$ g L^{-1} and different coating wet thicknesses on mica (from left to right: 250, 500, and 1000 μm, respectively) (scale bar = 20 μm).

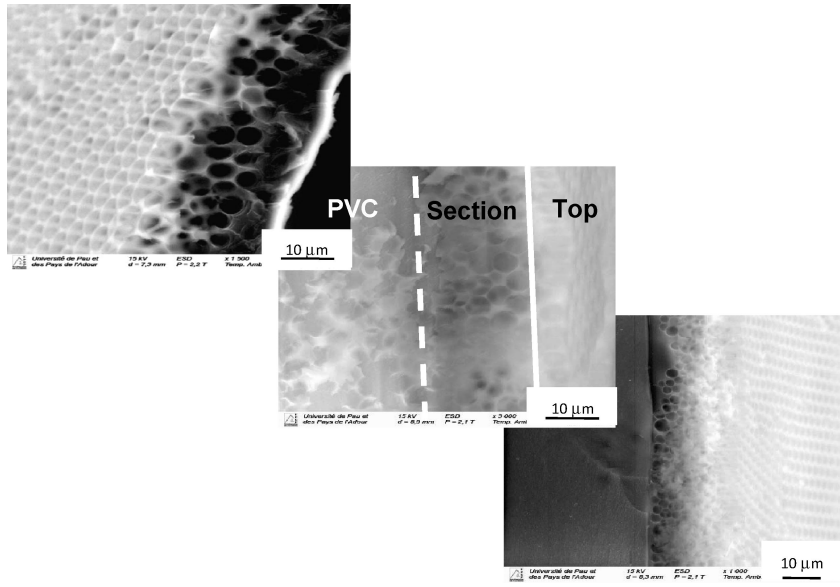

Figure 7. SEM images of cross section of polystyrene honeycomb structured film on mica, PVC sheet, and PMMA plate, from a polymer solution concentration $C_p = 10$ g L^{-1} (from top to bottom, respectively) (scale bar = 10 μm).

Scheme 3. Geometrical and Naming Conventions for Grating Description: (a) Reflection; (b) Transmission

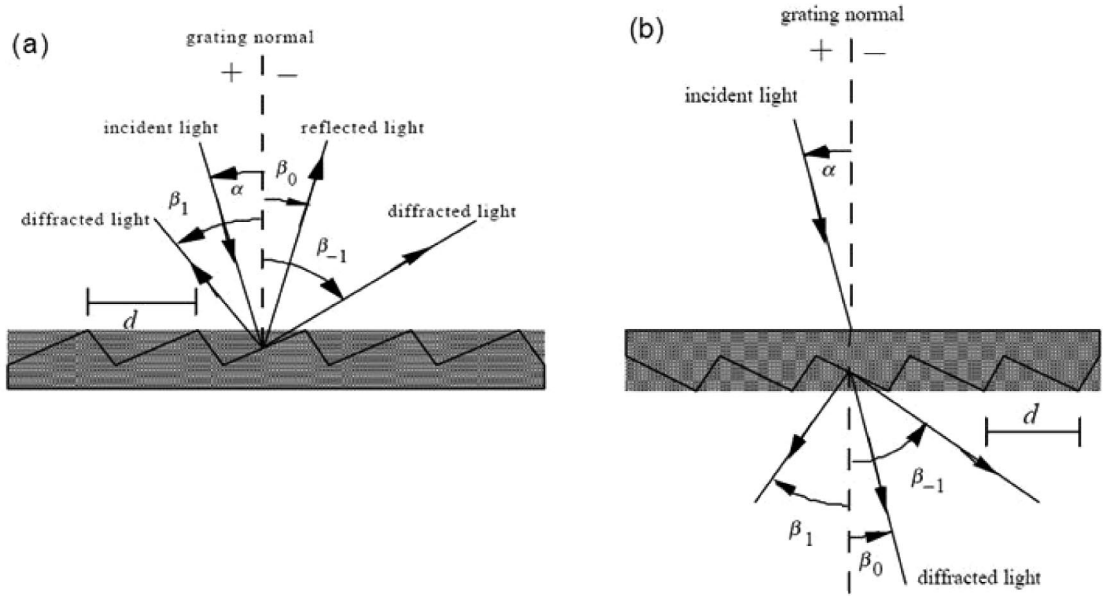

have been cast from a high polymer concentration ($C_p = 10$ g L^{-1}) and wet thickness (1000 μm) on various substrates to visualize the 3-dimensional (3D) organization. The SEM images of the cross section given in Figure 7 reveal the formation of a multilayer ordered structure, as expected. Indeed, we can visualize a 3D array on a thickness of 25 μm from PS film disconnected from the mica surface by simple immersion in water. The same structured films are observed onto polymeric substrates such as PVC or PMMA. In this case, we have observed a strong adhesion of the films obtained from the anionic ionomeric macromolecular design.

The strong adhesion of the PS honeycomb film on the PVC sheet is observed in Figure 7 (middle). Indeed, we can remark on the presence of residual broken pores still anchored or partially adsorbed to the PVC substrate. In case of the PMMA plate, a clean break is observed with strong cohesiveness between the honeycomb structured film and the substrate. It seems that such anionic ionomer behaves differently with the nature of the substrate. For mica, it is well-known that the surface is very hydrophilic and negatively charged, and thus some electrostatic repulsions can occur with the highly structured film based on negatively end-charged group. On the other hand, we recently demonstrated that the cationic end-group of the PS described in Table 1 interacts strongly to the mica surface.[22] On the contrary, the PVC/PMMA substrates present some polarized C−Cl and C═O dipoles able to strongly react and promote adhesion with the anionic monochelic PS chains.

Srinivasarao et al. have shown that the formation of multilayered structures arises from the consecutive sinking of condensed water droplets into the sample solution.[17] The formation of mono- and multilayer structures was proposed to depend on the solvent density. Multilayer structures were usually found from the solvents with densities lower than water. But under our experimental conditions, even if the carbon disulfide has a higher density than water, a multilayer structure has been observed. Such a phenomenon has also been reported by François et al.[2] which mentioned the impact of the deposited volume to create 3D arrangement, as described in the previous

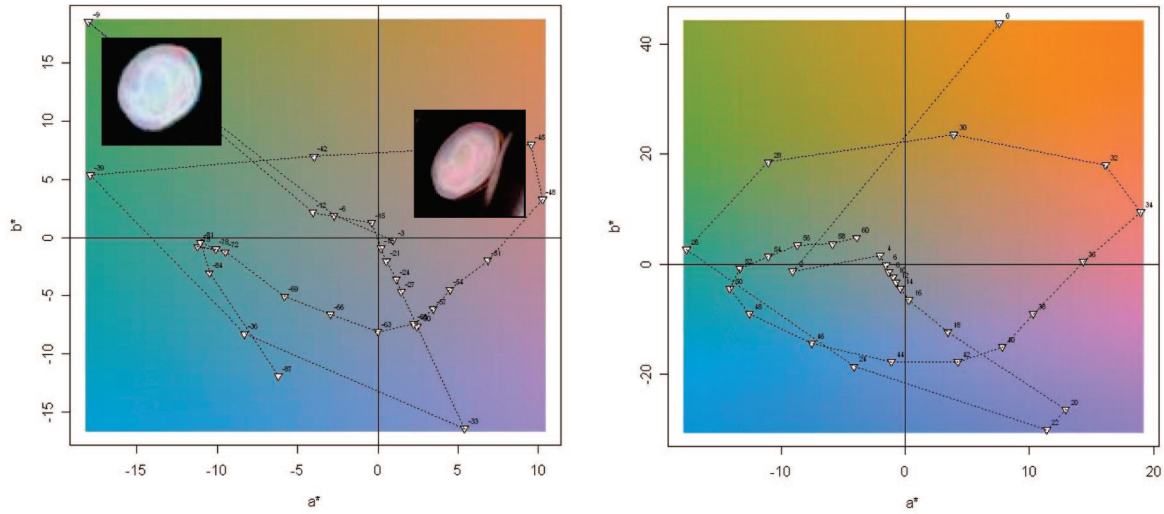

Figure 8. Chromaticity plots (CIELab color space) for sample S1 in reflection (R) and transmission (T) from left to right, respectively (insets: photographs of the color evolution at the approximate reflection angles 10° and 45° and positioned in their respective color area).

section. Qiao et al. mentioned if the water microspheres are smaller than the thickness of the deposited droplet of polymer solution, then multiple layers are formed.[5b] Nevertheless, the formation of arrays of holes ordered in a honeycomb structure has not been fully elucidated even though several papers have been published on this subject. Moreover, due to the complexity of the phenomenon and number of specific experimental parameters, its full understanding and well-controlled elaboration are not yet perfectly achieved.

But in the present case, if the multilayered films are due to consecutive dives of condensed water droplets, the size of the pores has to be the same on the top and inside the films. Herein, we used a grating model based on reflection and transmission of light as a pore size approximation.[30] Two samples cast under controlled conditions of temperature ($T = 25$ °C) and polymer concentration ($C_p = 10$ g L^{-1}) with different air humidity (45% and 60%) have been studied to tune the pores size.

Under the hypothesis that the honeycomb structures would behave as gratings, diffraction properties allow computing of an estimated periodicity using the Grating equation:

$$m\lambda = d(\sin \alpha + \sin \beta) \quad (1)$$

where m is the diffraction order, λ is the wavelength, d is the groove spacing, α is the incident angle, and β is the diffraction angle as given in Scheme 3.

The luminous intensities diffracted by two honeycomb structures were measured in both reflection and transmission using a goniospectroradiometer. Moreover, besides the highly ordered hexagonal pattern of these materials, we have observed other phenomena: a color diffraction which can be originated from the regularity of such honeycomb structured surface obtained from ionomer macromolecular systems. This micro-sized patterned honeycomb structure decomposes the white light or sunlight and creates a rainbow on the flat surface. This interferential optical phenomenon can be created by a simple tilt of the coating to diffract the light.[19] A more precise study can be achieved using spectrophotogoniometry. Indeed, it is possible to check the interferential optical phenomena and the decomposition of the white light which interferes with a structured surface. Figure 8 represents a plot of the chromaticity coordinates of the reflected and transmitted lights.

The crossings of the chromatic trajectory (same chromaticity for two different angles) correspond to different values of m. Chromatic trajectories obtained from optical quality, ruled gratings generally appear as spiral paths around the achromatic point, i.e., origin of both axes of the graph (as observed with a standard Micro-Control-Newport plane). Points belonging to increasing refraction orders appear as radius-aligned points of decreasing saturation. While industrial gratings are designed for use either in reflection or transmission and only have a surface texture, our materials have a 3D structure leading to the observed imperfect patterns.

Table 2. Honeycomb Films 3-Dimensional Properties as a Function of Air Humidity

		$d_{calculated}$ (μm)		$d_{measured}$ (μm)		d_2/d_1		
sample	humidity (%)	reflected light	transmitted light	SEM	DLD	grating	SEM	DLD
S1	45	1.16	1.16	1.22	1.08	1.32	1.20	1.17
S2	60	1.52	1.54	1.44	1.26			

Such highly ordered hexagonal pattern presents a strong angular dependence. We can observe that the color perception of such structured surface can be highly shifted from blue through green and orange to purple by playing with the angle of observation. The common optical pathway does not change so much in reflection compared to transmission. The same conclusion can be realized from the effect of the pores size in the micron-sized range (see Supporting Information).

In this case, the high interferential effect is obtained due to the strong diffraction of the light onto this highly structured system and can be used to tune perception of colored surface as with pure inorganic pearlescent pigments.

Table 2 gives the values of d, corresponding to the distance between pore centers that are obtained by different approaches such as resolving eq 1, SEM, or diode laser diffraction (DLD) pattern. The table shows that the calculated distance between pore centers is in good accordance with the distance measured in the horizontal plane on SEM images (Figure 9). Independent calculations using data collected under reflected or transmitted light lead to identical size determinations in the horizontal and vertical directions, confirming an isotropic structure close to a hexagonal compact configuration. Sample S2 exhibits a 20−30% increase of the distance between pore centers compared to sample S1 ($d_2/d_1 = 1.2$ and 1.32 by SEM and grating model, respectively). This phenomenon is directly correlated with the size of the condensed water droplets onto the polymer solution/air interface when hygrometry increased from 45 to 60%. This behavior was confirmed by the pore size of 3 μm obtained in the first part of this study, when the air humidity was 85%.

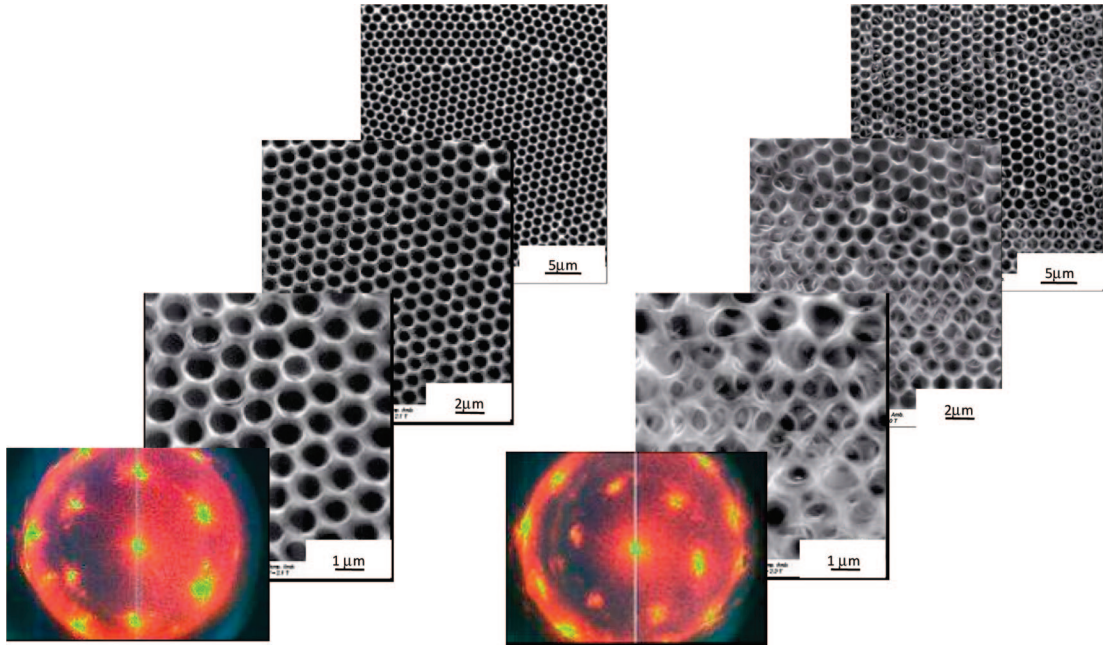

Figure 9. Laser diffraction patterns and SEM images of honeycomb structured films S1 (left) and S2 (right) as a function of air humidity (scale bar = 1, 2, and 5 μm from bottom to top, respectively).

Scheme 4. Mechanism of Breath Figure Arrays (BFA) Formation in 3D by the Bottom-Up Approach

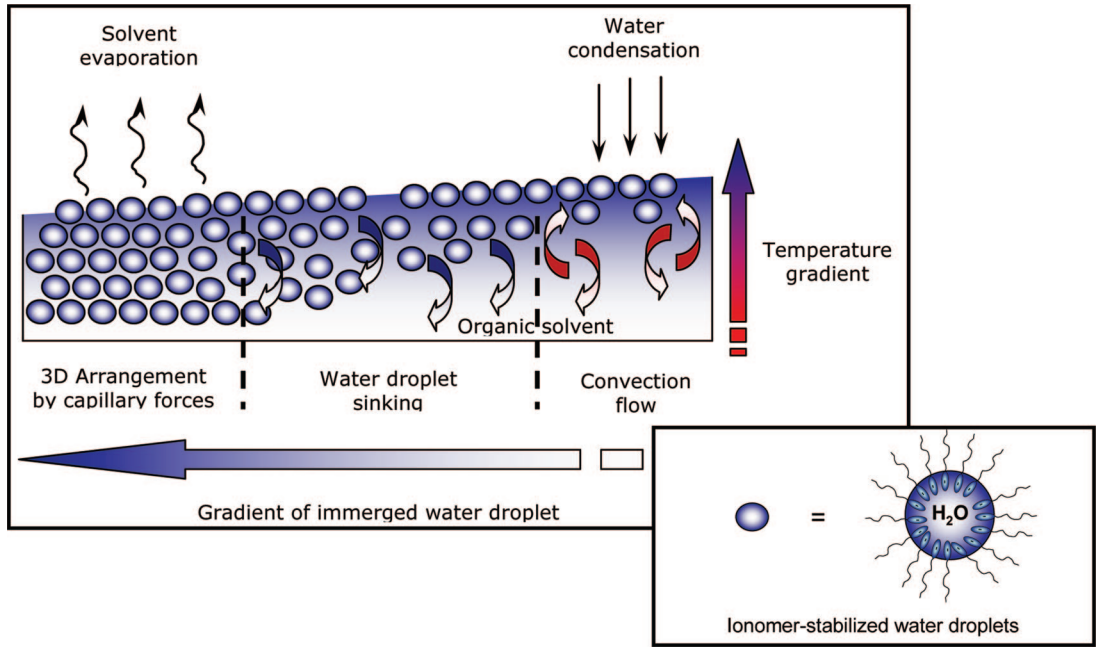

The ordered arrangement of micropores was clearly indicated by a light scattering experiment or laser diffraction pattern obtained in Figure 9. A red diode laser with a wavelength of 637 nm was used as a light source. The diffraction pattern was projected on a detector of a web camera. The use of this technique as a clever way of characterizing BF has been already demonstrated.[31] A diffraction pattern with hexagonally arranged spots was obtained from the honeycomb-patterned film S1 and S2. According to Bragg's law, i.e., $m\lambda = 2d \sin \theta$, where λ is the wavelength of the incident light, d is the lattice constant of the scattering centers, and θ is the angle of diffraction, the lattice constant d was calculated as a function of the CCD frame. The average lattice constant of the micropore was calculated as 1.08 and 1.26 μm for S1 and S2, respectively. These values were consistent with the distance between pore centers estimated from grating model and SEM. The view of the subsequent order, i.e., in the outer corona of the detector, indicates that the micropores lattice in the film has a highly ordered hexagonal arrangement, as confirmed by SEM.

Here a simple grating model shows to be useful in tailoring pore size for specific optical behavior of the honeycomb structure onto the surface but also inside the films. Moreover, the pore size calculated from reflected (surface) and transmitted (bulk) light are strictly the same and confirmed by the LD measurements. Such phenomena mean that the created pores, inside and on the top of the films, have the same dimensions and are due to the consecutive sinking of the condensed water droplets. The consecutive sinking of the condensed water droplets could be due to the Bènard−Marangoni convection and thermocapillary effect which forced the water droplets circula-

tion inside the polymer solution. Indeed, when the wet thickness is sufficiently high, i.e., much higher than the condensed water droplets, these last ones could dive inside the solution dragging down by the thermal convection flow (Scheme 4).

The model is consistent with the SEM observation of sample cross section and the LD patterns, as illustrated in Figures 7 and 9, which means that this optical approach permits to obtain a good correlation of the pores size estimation inside and on the top of the highly ordered hexagonal arrangements of the honeycomb films.

In a recent review paper, Bunz claims that in the beginning steps droplets can be considered either in "levitation" or as touching of the surface or submerged in the solvent.[1] We demonstrated, here, even with a high density solvent, the formation of a multilayer ordered structure. In the present case, after condensation and ordering, the successive water droplets layer dip and stay in levitation into the CS_2 solution, while it is impossible to invoke polymer/substrate interactions at this stage because the polymer and the substrate are both negatively charged (no different specific attractions can be invoked but rather electrostatic repulsions between negatively charged mica and ionomer macromolecules used in this study). The droplets cannot reach the substrate surface due to the strong anionic repulsion between the surface and anionic terminated macromolecules, and after complete evaporation, the substrate is coated with a homogeneous polymer thin layer. The successive highly ordered water droplets layers seem to be shifted of a half array to create the more compact arrangement, i.e., a centered hexagonal pattern (Figure 7). This model is in agreement with the Shimomura's mechanism.[32] Indeed, they claimed that the initial water droplets neither levitate nor are ordered on the surface, but thermocapillary and Marangoni forces cause the water droplets to submerge into the organic solution. Moreover, Bormashenko has recently demonstrated that Rayleigh and Marangoni numbers featuring instabilities occurring in liquid layers deposited on solid substrates and exerted to temperature gradients are sensitive to the thickness of the substrate.[33] The thermocapillary and Marangoni forces, which are exerted on the submerged droplets due to the temperature gradients, could then be responsible for the observed hexagonal order. In our study, we clearly demonstrated by SEM and optical methods that is possible to successively assemble and stack many hexagonal ordered layers due to the controlled and high wet thickness of the polymer solution.

This unusual optical approach is very powerful due to its ability for giving us some color information based on light diffraction but also some parameters of the internal constitution of highly ordered honeycomb surfaces such as breath figure films by light transmission. This highly ordered hexagonal pattern on inorganic or polymeric surfaces suggests the possibility of taking advantage of the microtextures for inducing optical interferences but also to modify the color of this bioinspired material as a function of their visual angle as in nature.

Conclusion

Nitroxide-mediated polymerization was found to be a suitable technique to generate functionalized polystyrene in a one-step process. The resulting polymer was successfully utilized to prepare highly regular honeycomb structured porous film. This process represents a versatile way of preparing films with a regular arrangement of pore diameters in a long-range distance (few hundred micrometers) on various substrates. The size of these structures can easily tailored by changing the polymer concentration or relative humidity. Moreover, the morphology of the honeycomb films can be easily tuned by the difference of the polymer solution thickness cast on the substrate. For a low MW as used here, the ionomer macromolecular design leads to a highly organized HC films. This behavior is associated with the self-assembly in organic solvent of the polar end-group and the direct consequence on the viscosity of the polymer solution.

The domain of applications is very large and has still to be explored, especially toward optical visual effects by creating bioinspired interferential and iridescent materials which offer new fascinating applications as original functional biomimetic coating on organic or inorganic surfaces.

Acknowledgment. We thank B. François and J. Francois for scientific discussions and special thanks to P. Maury from 2PSM "Propriétés Psychosensorielles des Matériaux" for his support and motivation. F. Roby and F. Ehrenfeld are acknowledged for their scientific/technical contribution for the laser diffraction setup. M.M. postdoc position of the GR2PSM "Biomimetic project" was financed by the Communauté d'Agglomération Pau-Pyrénées CDAPP.

Supporting Information Available: Figure showing the chromaticity plots for sample S2 in reflection (R) and transmission (T). This material is available free of charge via the Internet at http://pubs.acs.org.

References and Notes

(1) Bunz, U. *Adv. Mater.* **2006**, *18*, 973–989.
(2) (a) Widawski, G.; Rawiso, M.; François, B. *Nature (London)* **1994**, *369*, 387–389. (b) François, B.; Pitois, O.; François, J. *Adv. Mater.* **1995**, *7*, 1041–1044.
(3) François, B.; Ederlé, Y.; Mathis, C. *Synth. Met.* **1999**, *103*, 2362–2363.
(4) Wong, K. H.; Hernandez-Guerrero, M.; Granville, A.; Davis, T. P.; Barner-Kowollik, C.; Stenzel, M. *J. Porous Mater.* **2006**, *13*, 213–223.
(5) (a) Stenzel, M. *Aust. J. Chem.* **2002**, *55*, 239–243. (b) Connal, L. A.; Gurr, P. A.; Qiao, G. G.; Solomon, D. H. *J. Mater. Chem.* **2005**, *15*, 1286–1292. (c) Connal, L. A.; Qiao, G. G. *Adv. Mater.* **2006**, *18*, 3024–3028. (d) Connal, L. A.; Qiao, G. G. *Soft Matter* **2007**, *3*, 837–839. (e) Connal, L. A.; Vestberg, R.; Gurr, P. A.; Hawker, C. J.; Qiao, G. G. *Langmuir* **2008**, *24*, 556–562.
(6) (a) Zhao, X. Y.; Cai, Q.; Shi, G. X.; Shi, Y. Q.; Chen, G. W. *J. Appl. Polym. Sci.* **2003**, *90*, 1846–1850. (b) Beattie, D.; Wong, K. H.; Williams, C.; Poole-Warren, L.; Davis, T. P.; Barner-Kowollik, C.; Stenzel, M. *Biomacromolecules* **2006**, *7*, 1072–1082.
(7) De Boer, B.; Stalmach, U.; Nijland, H.; Hadziionannou, G. *Adv. Mater.* **2000**, *12*, 1581–1583.
(8) Karthaus, O.; Cieren, K.; Maryuama, N.; Shimomura, M. *Mater. Sci. Eng* **1999**, *10*, 103–106.
(9) Sun, H.; Li, H.; Bu, W.; Xu, M.; Wu, L. *J. Phys. Chem. B* **2006**, *110*, 24847–24854.
(10) Xia Cheng, C.; Tian, Y.; Qiao Shi, Y.; Pei, R.; Xi, F. *Langmuir* **2005**, *21*, 6576–6581.
(11) (a) Wong, K. H.; Davis, T. P.; Barner-Kowollik, C.; Stenzel, M. *Aust. J. Chem.* **2006**, *59*, 539–543. (b) Böker, A.; Lin, Y.; Chiapperini, K.; Horowitz, R.; Thompson, M.; Carreon, V.; Xu, T.; Abetz, C.; Skaff, H.; Dinsmore, A. D.; Emrick, T.; Russell, T. P. *Nat. Mater.* **2004**, *3*, 302–306.
(12) Bormashenko, E.; Pogreb, R.; Stanevsky, O.; Bormashenko, Y.; Socol, Y.; Gendelman, O. *Polym. Adv. Technol.* **2005**, *16*, 299–304.
(13) Nishikawa, T.; Ookura, R.; Nishida, J.; Arai, K.; Hayashi, J.; Kurono, N.; Sawadaishi, T.; Hara, M.; Shimomura, M. *Langmuir* **2002**, *18*, 5734–5740.
(14) Zander, N. E.; Orlicki, J. A.; Karikari, A. S.; Long, T. E.; Rawlett, A. M. *Chem. Mater.* **2007**, *19*, 6145–6149.
(15) (a) Peng, J.; Han, Y.; Yang, Y.; Li, B. *Polymer* **2004**, *45*, 447–452. (b) Cui, L.; Peng, J.; Ding, Y.; Li, X.; Han, Y. *Polymer* **2005**, *46*, 5334–5340.
(16) Bolognesi, A.; Mercogliano, C.; Yunus, S.; Civardi, M.; Comoretto, D.; Turturro, A. *Langmuir* **2005**, *21*, 3480–3485.
(17) Srinivasarao, M.; Collongs, D.; Philips, A.; Patel, S. *Science* **2001**, *292*, 79–83.
(18) Park, M. S.; Kim, J. K. *Langmuir* **2004**, *20*, 5347–5352.
(19) (a) Ghannam, L.; Garay, H.; François, J.; Billon, L. *Macromol. Chem. Phys.* **2007**, *208*, 1469–1479. (b) Ghannam, L.; Manguian, M.; Francois, J.; Billon, L. *Soft Matter* **2007**, *3*, 1492–1499.

(20) Zhong, X. F.; Eisenberg, A. *Macromolecule* **1994**, *27*, 1751–1758.
(21) (a) Karaky, K.; Pere, E.; Pouchan, C.; Desbrières, J.; Derail, C.; Billon, L. *Soft Matter* **2006**, *2*, 770–778. (b) Karaky, K.; Pere, E.; Pouchan, C.; Garay, H.; Khoukh, A.; Desbrières, J.; Francois, J.; Billon, L. *New J. Chem.* **2006**, *30*, 698–705. (c) Karaky, K.; Billon, L.; Pouchan, C.; Desbrières, J. *Macromolecules* **2007**, *40*, 458–464. (d) Karaky, K.; Clisson, G.; Reiter, G.; Billon, L. *Macromol. Chem. Phys.* **2008**, *209*, 715–722.
(22) (a) Ghannam, L.; Garay, H.; Bacou, M.; Francois, J.; Shanahan, M. E. R.; Billon, L. *Polymer* **2004**, *45*, 7035–7045. (b) Ghannam, L.; Garay, H.; Francois, J.; Shanahan, M. E. R.; Billon, L. *Chem. Mater.* **2005**, *17*, 3837–3843. (c) Ghannam, L.; Garay, H.; Billon, L. *Macromolecules* **2008**, *41*, 7374–7382.
(23) Stenzel, M.; Barner-Kowollik, C.; Davis, T. P. *J. Polym. Sci., Part A: Polym. Chem.* **2006**, *44*, 2363–2375.
(24) (a) Yunus, S.; Delcorte, A.; Poleunis, C.; Bertrand, P.; Bolognesi, A.; Botta, C. *Adv. Funct. Mater.* **2007**, *17*, 1079–1084. (b) Stenzel, M.; Davis, T. P. *Aust. J. Chem.* **2003**, *56*, 1035–1038. (c) Yabu, H.; Shimomura, M. *Langmuir* **2006**, *22*, 4992–4997.
(25) Karthaus, O.; Maryuama, N.; Cieren, K.; Shimomura, M.; Hasegawa, H.; Hashimoto, T. *Langmuir* **2000**, *22*, 6071–6076.
(26) (a) Williams, C. E.; Russell, T. P.; Jérôme, R.; Horrion, J. *Macromolecules* **1986**, *19*, 2877–2884. (b) Broze, G.; Jérôme, R.; Teyssié, Ph. *Macromolecules* **1982**, *15*, 920–927.
(27) Gao, Z.; Zhong, X. F.; Eisenberg, A. *Macromolecules* **1994**, *27*, 794–802.
(28) Eisenberg, A.; Hird, B.; Moore, R. B. *Macromolecules* **1990**, *23*, 4098–4107.
(29) Min, E.; Wong, K. H.; Stenzel, M. H. *Adv. Mater.* **2008**, *9999*, 1–7.
(30) Benisty, H.; Berger, V.; Gerard, J. M.; Maystre, D.; Tchelnokov, A. In *Photonic Crystals Towards Nanoscale Photonic Devices*; Louritioz, J. M., Ed.; Springer: Berlin, 2005; p 63.
(31) (a) Bolognesi, A.; Botta, C.; Yunus, S. *Thin Solid Films* **2005**, *492*, 307–312. (b) Yabu, H.; Tanaka, M.; Ijiro, K.; Shimomura, M. *Langmuir* **2003**, *19*, 6297–6300. (c) Yabu, H.; Shimomura, M. *Langmuir* **2005**, *21*, 1709–1711.
(32) Maruyama, N.; Koito, T.; Nishida, J.; Sawadaishi, T.; Cieren, X.; Kjiro, K.; Karthaus, O.; Shimomura, M. *Thin Solid Films* **1998**, *327*, 854–856.
(33) Bormashenko, E. *Ind. Eng. Chem. Res.* **2008**, *47*, 1726–1728.

MA8020568